Global polarization of Λ, Ξ^-, and Ω^- hyperons in Au+Au collisions at RHIC BES-II energies

Gen-Hui Li,[1,*] Cong Yi,[2,†] Xiang-Yu Wu,[3,‡] Shi Pu,[1,4,§] and Guang-You Qin[2,¶]

[1] *Department of Modern Physics, University of Science and Technology of China, Anhui 230026, China*
[2] *Institute of Particle Physics and Key Laboratory of Quark and Lepton Physics (MOE), Central China Normal University, Wuhan 430079, China*
[3] *Department of Physics, McGill University, Montreal, QC, Canada H3A 2T8*
[4] *Southern Center for Nuclear-Science Theory (SCNT), Institute of Modern Physics, Chinese Academy of Sciences, Huizhou 516000, Guangdong Province, China*

We investigate the global spin polarization of Λ hyperons and the multi-strange hyperons Ξ^- and Ω^- in Au+Au collisions across the RHIC Beam Energy Scan II (BES-II) energy range, $\sqrt{s_{NN}} = 7.7$–27 GeV. The polarization is computed using the modified Cooper–Frye formula, which includes contributions from thermal vorticity, the thermal shear tensor, and the gradient of the baryon chemical potential, combined with the (3+1)-dimensional viscous hydrodynamic framework CLVisc with SMASH initial conditions. We present the global polarization as a function of collision energy, centrality, transverse momentum, and rapidity. We find that the global polarization of Ω^- is systematically larger than those of Λ and Ξ^- because of its larger spin quantum number, but it remains below the central value of the recent STAR measurement. This discrepancy may suggest that additional mechanisms, such as spin correlations among strange quarks inside the Ω^-, could contribute to the observed Ω^- polarization. We also find that the global-polarization splitting between hyperons and anti-hyperons increases toward lower collision energies and is dominated by the chemical-potential-gradient contribution.

I. INTRODUCTION

In noncentral relativistic heavy-ion collisions, the quark-gluon plasma (QGP) created in the overlap region carries enormous orbital angular momentum and behaves as the most vortical fluid observed so far, with an angular velocity reaching up to 10^{22} s^{-1} [1]. Such an immense vorticity can polarize the spins of final-state hadrons along the direction of the initial orbital angular momentum through spin–orbit coupling [2, 3]. This phenomenon is known as global spin polarization in relativistic heavy-ion collisions. Over the past decade, the global polarization of Λ and $\bar{\Lambda}$ hyperons has been extensively measured from a few GeV up to the TeV scale and in different collision systems [1, 4–9]. On the theoretical side, numerical calculations based on the spin-polarization vector derived from the quantum statistical model [10] or from quantum kinetic theory [11] have described the collision-energy dependence of the global polarization of Λ hyperons over $\sqrt{s_{NN}} = 7.7$–200 GeV [10–29]. At low collision energies, the global polarization of Λ hyperons is found to continue increasing as the collision energy decreases [5, 30]. Although several studies have investigated the effects of vorticity [31–34], the mechanism underlying the global polarization at such low collision energies is still not fully understood. Very recently, the global polarization of hypernuclei and protons has also been studied [35–38].

Although significant progress has been made, several issues concerning global polarization remain to be understood. First, most existing studies have focused on the collision-energy dependence of the global polarization, while its dependence on rapidity, centrality, and transverse momentum still requires further investigation, especially in view of future experimental measurements. Second, it has been found that the polarization induced by the shear tensor and by the gradient of the baryon chemical potential [39–50], which are closely related to spin Hall-type effects, can affect the polarization of hyperons along the beam direction [33, 51–63]. Therefore, a natural question is how large the contributions from shear-induced polarization and spin Hall effects are to the global polarization. Third, the polarization of multi-strange hyperons [64] has also attracted considerable attention. These particles provide a useful probe of whether spin correlations [65–84] exist among strange quarks inside a hyperon and, if so, how such correlations affect the observed global polarization. This remains an open issue that calls for systematic theoretical investigation. Finally, the origin of the global-polarization splitting between hyperons and anti-hyperons remains unclear. Besides the splitting induced by electromagnetic fields [85–89], gradients of the chemical potential can also contribute to this splitting [28, 46]. Therefore, it is important to clarify the relative contributions of these different mechanisms.

Interestingly, the high-statistics data from the RHIC Beam Energy Scan II (BES-II) [91] are expected to provide more precise measurements of both the global polarization of multi-strange hyperons. Therefore, it is timely to study the global polarization at the new collision en-

* genhuili@mail.ustc.edu.cn
† congyi@mail.ustc.edu.cn
‡ xiangyu.wu2@mail.mcgill.ca
§ shipu@ustc.edu.cn
¶ guangyou.qin@ccnu.edu.cn

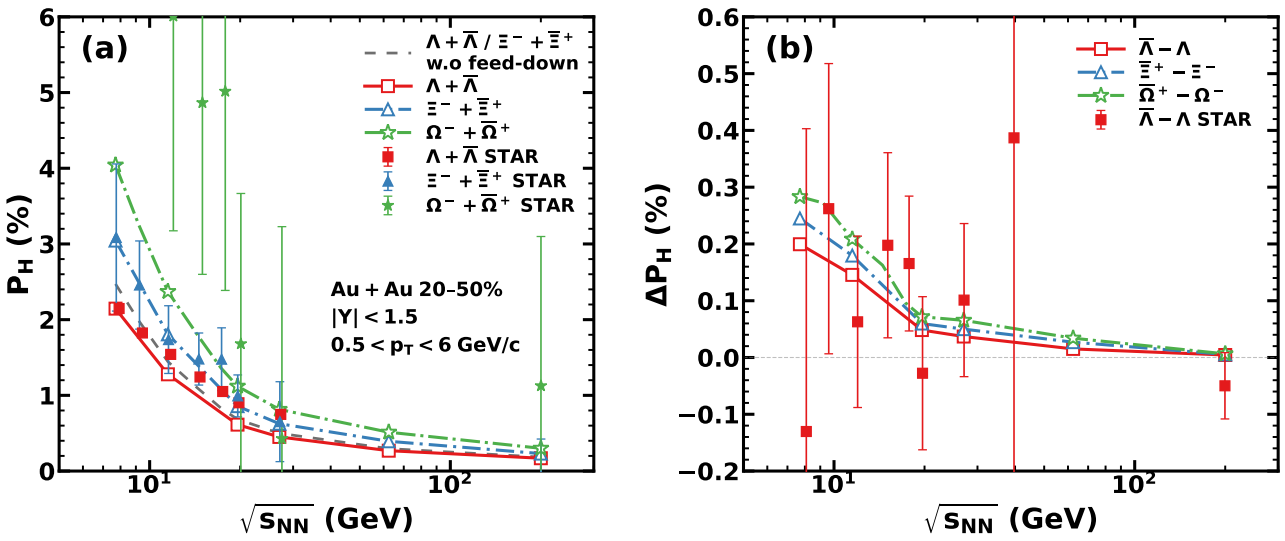


Figure 1. (a) Global polarization P_H and (b) global-polarization splitting ΔP_H of Λ, Ξ^-, and Ω^- hyperons in 20–50% central Au+Au collisions as functions of collision energy. The rapidity and transverse-momentum ranges are set to $|Y| < 1.5$ and $0.5 < p_T < 6$ GeV/c, respectively. Red filled squares, blue filled triangles, and green filled stars represent the experimental data points for the global polarization of Λ, Ξ, and Ω extracted from Ref. [90], respectively. Open symbols with the same colors represent the corresponding theoretical results.

ergies covered by BES II.

To address these issues and provide predictions for global polarization in the RHIC BES-II energy range, we employ the (3+1)-dimensional hydrodynamic framework CLVisc [92–94], with SMASH initial conditions [95–101], to compute the global polarization of the multi-strange hyperons Ξ^- and Ω^-, together with the hyperon–anti-hyperon polarization splitting and the corresponding feed-down effects, at $\sqrt{s_{NN}} = 7.7$–27 GeV.

This paper is organized as follows. In Secs. II and III, we introduce the theoretical framework and the numerical setup, respectively. In Sec. IV, we present our numerical results for the global polarization of Λ, Ξ^-, and Ω^- hyperons and analyze its dependence on collision energy, centrality, transverse momentum, and rapidity. Finally, we summarize our findings in Sec. V.

II. THEORETICAL FRAMEWORK

In this section, we briefly describe our theoretical framework. Based on the quantum statistical model [10] or quantum kinetic theory [11], the mean spin-polarization vector of spin-s fermions, normalized by the particle number and the spin quantum number, is given by

$$\mathcal{P}^\mu(\mathbf{p}) = \frac{(s+1)\int d\Sigma\cdot p\,\mathcal{J}_5^\mu(p,x)}{3m_f\int d\Sigma\cdot p\,f_{\rm eq}}, \tag{1}$$

where m_f is the fermion mass entering the normalization of the Pauli–Lubanski pseudovector, p^μ is the on-shell four-momentum of the fermion satisfying $p^2 = m_f^2$, and $f_{\rm eq} = \exp[(p^\alpha u_\alpha - \mu)/T] + 1^{-1}$ is the Fermi–Dirac distribution with flow velocity u_α, chemical potential μ, and temperature T. The vector $d\Sigma^\mu$ denotes the normal vector of the freeze-out hypersurface. The quantity $\mathcal{J}_5^\mu$ denotes the axial current in phase space, which is proportional to the spin current in phase space. Substituting $\mathcal{J}_5^\mu$ up to order $\hbar$ and neglecting electromagnetic fields, one can decompose $\mathcal{P}^\mu$ as [28, 45],

$$\mathcal{P}^\mu = \mathcal{P}^\mu_{\rm thermal} + \mathcal{P}^\mu_{\rm th\text{-}shear} + \mathcal{P}^\mu_{\rm chemical}, \tag{2}$$

with

$$\begin{aligned}
\mathcal{P}^\mu_{\rm thermal}(\mathbf{p}) &= \frac{s+1}{6m_f}\int d\Sigma\cdot\mathcal{N}_p\,\epsilon^{\mu\nu\alpha\beta}p_\nu\varpi_{\alpha\beta},\\
\mathcal{P}^\mu_{\rm th\text{-}shear}(\mathbf{p}) &= \frac{s+1}{3m_f}\int d\Sigma\cdot\mathcal{N}_p\,\frac{\epsilon^{\mu\nu\alpha\beta}p_\nu n_\beta}{(n\cdot p)}p^\sigma\xi_{\sigma\alpha},\\
\mathcal{P}^\mu_{\rm chemical}(\mathbf{p}) &= \frac{s+1}{3m_f}\int d\Sigma\cdot\mathcal{N}_p\,\frac{\epsilon^{\mu\nu\alpha\beta}p_\alpha}{(u\cdot p)}u_\beta\partial_\nu\frac{\mu}{T},
\end{aligned} \tag{3}$$

where $\mathcal{N}_p^\mu = p^\mu f_{\rm eq}(1 - f_{\rm eq})/\int d\Sigma\cdot p\,f_{\rm eq}$. The subscripts "thermal", "th-shear", and "chemical" label the contributions from the thermal vorticity $\varpi_{\alpha\beta} = \frac{1}{2}[\partial_\alpha(u_\beta/T) - \partial_\beta(u_\alpha/T)]$, thermal shear tensor $\xi_{\alpha\beta} = \frac{1}{2}[\partial_\alpha(u_\beta/T) + \partial_\beta(u_\alpha/T)]$, and chemical-potential gradient $\nabla(\mu/T)$, respectively.

To compare with experimental measurements, we further boost the polarization vector $\mathcal{P}^\mu$ to the rest frame of the particle,

$$\vec{\mathcal{P}}_*(\mathbf{p}) = \vec{\mathcal{P}}(\mathbf{p}) - \frac{\vec{\mathcal{P}}(\mathbf{p})\cdot\vec{p}}{p^0(p^0+m)}\vec{p}, \tag{4}$$

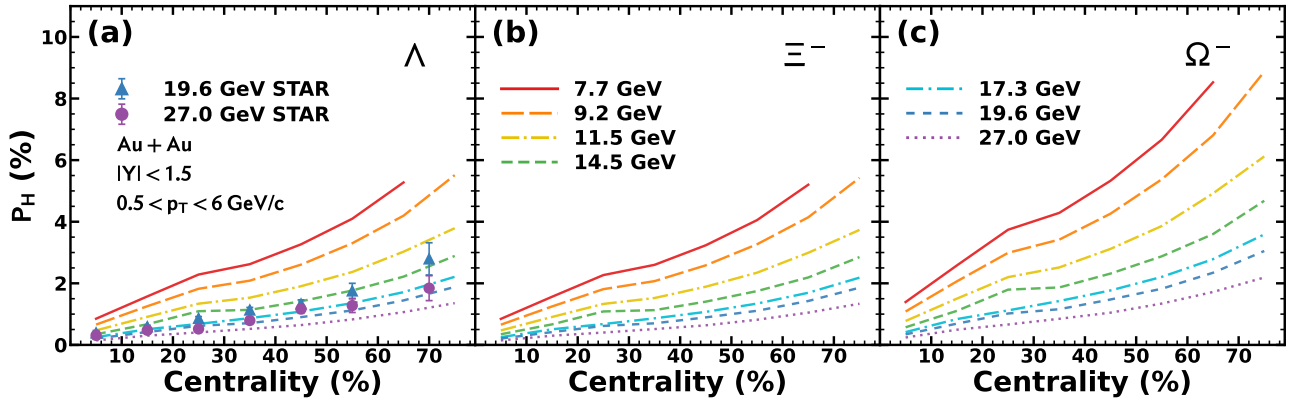


Figure 2. Global polarization P_H of (a) Λ, (b) Ξ^-, and (c) Ω^- hyperons in Au+Au collisions as a function of centrality at different collision energies. The rapidity and transverse-momentum ranges are set to $|Y| < 1.5$ and $0.5 < p_T < 6$ GeV/c, respectively. The blue filled triangles and purple filled circles represent the experimental data points for the global polarization of Λ at 19.6 and 27.0 GeV extracted from Ref. [8], respectively. Lines with different colors and styles represent the theoretical results at different collision energies.

and define the particle-number-weighted observables for the global polarization along the $-y$ direction as

$$P_H = -\frac{\int p_T dp_T dY d\phi_p \int d\Sigma \cdot p\, f_{\rm eq} \mathcal{P}_*^y}{\int p_T dp_T dY d\phi_p \int d\Sigma \cdot p\, f_{\rm eq}}, \quad (5)$$

where p_T is the transverse momentum, while ϕ_p and Y are the azimuthal angle and rapidity of the particle momentum, respectively. We also define the p_T- and Y-dependent global polarization as

$$P_H(p_T) = -\frac{\int dY d\phi_p \int d\Sigma \cdot p\, f_{\rm eq} \mathcal{P}_*^y}{\int dY d\phi_p \int d\Sigma \cdot p\, f_{\rm eq}},$$
$$P_H(Y) = -\frac{\int p_T dp_T d\phi_p \int d\Sigma \cdot p\, f_{\rm eq} \mathcal{P}_*^y}{\int p_T dp_T d\phi_p \int d\Sigma \cdot p\, f_{\rm eq}}. \quad (6)$$

For convenience, we also define the global-polarization splitting between hyperon H and its antiparticle $\bar{H}$ as

$$\Delta P_H \equiv P_{\bar{H}} - P_H. \quad (7)$$

III. NUMERICAL SETUPS

In this section, we introduce the numerical setup used in this work. We implement the (3+1)-dimensional hydrodynamic framework CLVisc with SMASH initial conditions to simulate the global spin polarization of Λ, Ξ^-, and Ω^- hyperons in 20–50% Au+Au collisions at $\sqrt{s_{NN}} = 7.7$–27 GeV.

Following our previous works [28, 102], the initial collision geometry and energy deposition are described by the hadronic transport model Simulating Many Accelerated Strongly-interacting Hadrons (SMASH) [95]. We collect all particles at the hydrodynamic initial proper time, which is approximated by the average nuclear overlap time as

$$\tau_0 = 2R/\sqrt{(\sqrt{s_{NN}}/2m_N)^2 - 1}. \quad (8)$$

Here, $R = 6.38$ fm is the average radius of the Au nucleus in the Woods–Saxon distribution, $\sqrt{s_{NN}}$ is the collision energy, and m_N is the nucleon mass. We then apply Gaussian smearing with a normalization factor K and smearing widths σ_r and σ_η in the transverse and longitudinal directions, respectively [28, 102], to generate the initial energy-momentum tensor $T_0^{\mu\nu}$ and the net-baryon current J_0^μ. Their subsequent evolution is described by the (3+1)-dimensional hydrodynamic framework CLVisc through the coupled energy-momentum and particle conservation equations.

In this work, we neglect bulk viscosity and set the baryon-diffusion coefficient to $C_B = 0$ for simplicity. We treat the specific shear viscosity C_{η_v} as a free parameter. These parameters are tuned to reproduce soft-particle yields and transverse-momentum spectra at $\sqrt{s_{NN}} =$ 7.7, 19.6, and 27 GeV. We find that a single set of Gaussian smearing parameters, K, σ_r, and σ_η, is sufficient to describe the spectra at all three collision energies, suggesting that the hadronic transport model provides a reasonable description of the initial energy deposition. This is consistent with the parameters used with the Ultra-Relativistic Quantum Molecular Dynamics (UrQMD) initial conditions in Ref. [103]. We therefore adopt the common Gaussian smearing parameters in our simulations, while choosing the same specific shear viscosity C_{η_v} as that used in Ref. [103]. All parameters used in the simulations are listed in Table I. Further details about the model and parameter choices can be found in Refs. [28, 92–95, 102].

To close the conservation equations, we use the NEOS-BQS equation of state [104, 105], which smoothly connects a hadron-resonance gas at finite chemical potential to lattice-QCD results through a Taylor-expansion method. The freeze-out energy density is chosen as $\epsilon_f = 0.4$ GeV/fm^3, corresponding to $T_f = 158$ MeV in the zero-chemical-potential limit. The relation between cen-

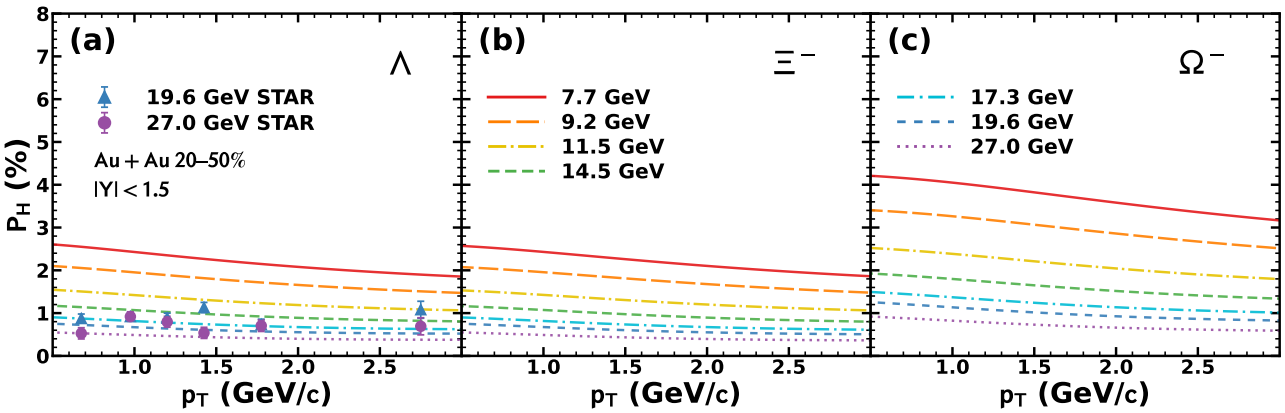


Figure 3. Global polarization P_H of (a) Λ, (b) Ξ^-, and (c) Ω^- hyperons in 20–50% central Au+Au collisions as a function of transverse momentum p_T at different collision energies. The rapidity is set to $|Y| < 1.5$. The blue filled triangles and purple filled circles represent the experimental data points for the global polarization of Λ at 19.6 and 27.0 GeV extracted from Ref. [8], respectively. Lines with different colors and styles represent the theoretical results at different collision energies.

Table I. Parameters used in the hydrodynamic simulations at different collision energies.

$\sqrt{s_{NN}}$ [GeV]	K	τ_0 [fm]	σ_r [fm]	σ_{η_s}	C_{η_v}
7.7	1.0	3.2	1.0	0.35	0.20
9.2	1.0	2.7	1.0	0.35	0.20
11.5	1.0	2.1	1.0	0.35	0.20
14.5	1.0	1.7	1.0	0.35	0.20
17.3	1.0	1.4	1.0	0.35	0.15
19.6	1.0	1.2	1.0	0.35	0.15
27	1.0	1.0	1.0	0.35	0.12

trality and impact parameter b is determined using the Monte Carlo Glauber model. In each centrality bin, we average over 5000 events to obtain a smooth initial condition. After the hydrodynamic evolution, we compute the global spin polarization according to Eq. (5, 6), using the same kinematic cuts as in the experimental measurements [8, 90]. The hyperon masses are $m_\Lambda = 1.116$ GeV, $m_\Xi = 1.322$ GeV, and $m_\Omega = 1.672$ GeV, and the corresponding spin quantum numbers are $S = 1/2$, $1/2$, and $3/2$, respectively. Therefore, within the same hydrodynamic background and polarization formula, the differences among the polarizations of these three hyperons mainly arise from their different masses and spin quantum numbers.

In experimental measurements, feed-down effects are included in the observed hyperon polarization. In this work, we follow Refs. [16, 18, 58, 59, 106, 107] to incorporate the feed-down effects.

IV. RESULTS AND DISCUSSION

We now discuss our results for the global polarization of Λ, Ξ^-, and Ω^- hyperons as functions of collision energy, centrality, transverse momentum, and rapidity.

In Fig. 1(a), we show the global polarization P_H as functions of collision energy for Λ, Ξ^-, and Ω^- hyperons We first observe that the global polarization of all three hyperon species increases as the collision energy decreases. This trend can be understood as a consequence of stronger net-baryon stopping, which deposits a larger fraction of the initial angular momentum into the produced medium, together with the smaller particle multiplicity near midrapidity at lower collision energies.

We next examine the global polarization of each hyperon species. For Λ and Ξ^- hyperons, since they have similar masses and the same spin quantum number, their primary polarizations computed from Eq. (1) are close to each other. On the other hand, according to Ref. [16, 18, 106, 107], feed-down effects enhance the Ξ^- polarization while reducing the Λ polarization. After including feed-down effects, our results for the global polarization of Ξ^- hyperons are consistent with the experimental data, while those for Λ hyperons are close to the data but slightly smaller at intermediate collision energies. We now discuss the global polarization of the Ω^- hyperon. Since the spin of the Ω^- hyperon is 3/2, Eq. (1) gives the simple estimate $P_\Omega \approx 5P_\Lambda/3$ if the mass difference between Ω^- and Λ and feed-down effects are neglected [2, 66, 67, 74]. Our numerical results are consistent with this estimate and show an enhancement of the global polarization of Ω^-. Nevertheless, our results remain well below the experimental central value, similar to earlier studies based on kinetic approaches [107]. This discrepancy may indicate that additional mechanisms, such as two- and three-particle spin-spin correlations among strange quarks inside the Ω^- hyperon, could contribute to the observed Ω^- polarization [66, 67, 74].

In Fig. 1(b), we present the global-polarization splitting ΔP_H as a function of collision energy. We find that anti-hyperons systematically carry a larger global polarization than the corresponding hyperons. This difference

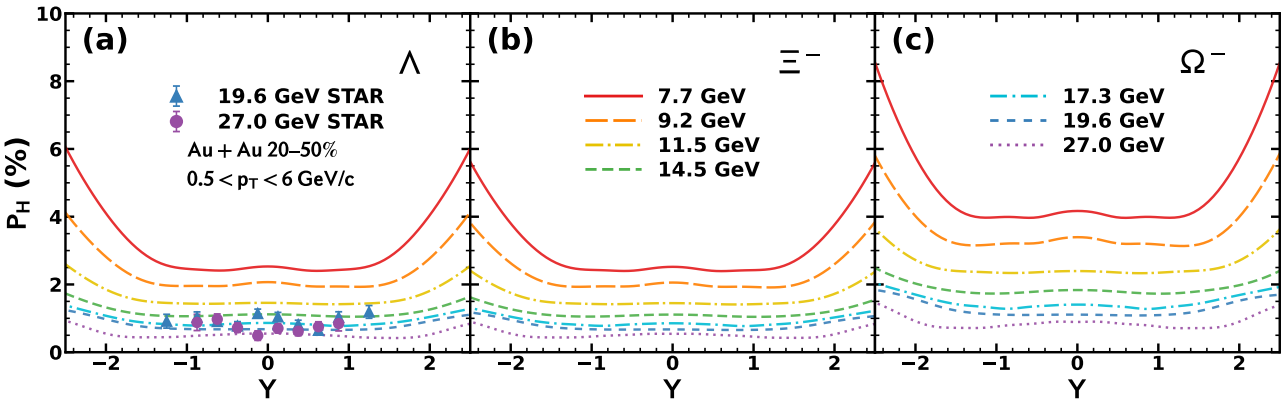


Figure 4. Global polarization P_H of (a) Λ, (b) Ξ^-, and (c) Ω^- hyperons in 20–50% central Au+Au collisions as a function of rapidity Y at different collision energies. The transverse-momentum ranges are set to $0.5 < p_T < 6$ GeV/c. The blue filled triangles and purple filled circles represent the experimental data points for the global polarization of Λ at 19.6 and 27.0 GeV extracted from Ref. [8], respectively. Lines with different colors and styles represent the theoretical results at different collision energies.

originates mainly from the chemical-potential-gradient contribution in Eq. (1). Therefore, a possible splitting of the global polarization between hyperons and anti-hyperons can arise not only from electromagnetic fields but also from the spin Hall effect. This finding is consistent with previous studies [46]. Our results for ΔP_Λ are consistent with the experimental data within uncertainties. We also provide predictions for ΔP_Ξ and ΔP_Ω.

Next, we present the global polarization of the three hyperon species as functions of centrality, transverse momentum p_T, and rapidity Y in Figs. 2, 3, and 4, respectively. Due to the lack of centrality-, p_T-, and Y-dependent feed-down corrections to the global polarization, we neglect feed-down effects for the remaining differential observables.

In Fig. 2, we observe that the centrality dependence of the global polarization of hyperons at intermediate collision energies is similar to that found at high collision energies [6, 7, 9, 64]. Namely, the polarization increases toward more peripheral collisions. This behavior can be attributed to the larger vorticity generated by stronger velocity gradients in more peripheral collisions, which enhances the global polarization. We also find that, at a fixed centrality, the global polarization becomes larger as the collision energy decreases, consistent with the collision-energy dependence shown in Fig. 1.

In Fig. 3, we observe that the global polarization decreases with increasing p_T. This trend is consistent with that observed in the experimental data. In Fig. 4, we also find that the global polarization of hyperons is nearly flat around midrapidity $|Y| \in [0, 1]$ and then increases rapidly with increasing $|Y|$ for $|Y| \geq 1$.

Comparing the global polarization of different hyperons in Figs. 2, 3, and 4, we observe that $P_\Xi \gtrsim P_\Lambda$ and $P_\Omega \simeq 5P_\Lambda/3$ at fixed collision energy, centrality, p_T, and Y, consistent with the spin and mass dependence in Eq. (1).

V. SUMMARY

In this work, we have studied the global spin polarization of Λ, Ξ^-, and Ω^- hyperons in 20–50% Au+Au collisions over $\sqrt{s_{NN}} = 7.7$–27 GeV, using the modified Cooper–Frye formula in Eq. (1) combined with the (3+1)-dimensional viscous hydrodynamic framework CLVisc with SMASH initial conditions.

We first show the global polarization of hyperons, P_H, as a function of collision energy in Fig. 1(a). We find that the global polarization of all three hyperon species increases as the collision energy decreases, in agreement with the trend observed by STAR. We observe a slight difference between the global polarizations of Ξ^- and Λ due to feed-down effects. In particular, feed-down effects enhance the global polarization of Ξ^- but reduce that of Λ. The global polarization of Ω^- is systematically larger than those of Λ and Ξ^- owing to its larger spin quantum number. Nevertheless, our result for the global polarization of Ω^- still underestimates the central value of the recent STAR measurement. This discrepancy may indicate the presence of two- and three-particle short-range spin correlations among the strange quarks inside the Ω^-.

In Fig. 1(b), we also present the global-polarization splitting ΔP_H as a function of collision energy. We find that the global polarization of anti-hyperons is larger than that of the corresponding hyperons. The splitting increases toward lower collision energies and is dominated by the chemical-potential-gradient contribution. Thus, the spin Hall effect can influence the global polarization in a way qualitatively similar to the electromagnetic-field contribution.

Finally, we plot the global polarization of hyperons as functions of centrality, transverse momentum p_T, and rapidity Y in Figs. 2, 3, and 4, respectively. For all three hyperon species, the global polarization increases to-

ward more peripheral collisions, decreases with increasing transverse momentum, and is nearly flat around midrapidity.

Our results provide a systematic theoretical baseline for the global polarization of multi-strange hyperons across the RHIC BES-II energy range. They also suggest that short-range spin correlations among strange quarks inside the Ω^- may be a promising direction for future theoretical and experimental investigation.

ACKNOWLEDGMENT

We would like to thank Zhenyu Chen, Xingrui Gou and Tong Fu for helpful discussion. This work is supported in part by the National Key Research and Development Program of China under Contract No. 2022YFA1605500, by the Chinese Academy of Sciences (CAS) under Grants No. YSBR-088 and by National Natural Science Foundation of China (NSFC) under Grant Nos. 12075235, 12225503, 11890710, 11890711, 11935007, 12175122, 2021-867, 11221504, 11861131009,12547164 and 11890714, by the China Postdoctoral Science Foundation under Grant Number 2025M783388. X.-Y.W. is supported in part by the Natural Sciences and Engineering Research Council of Canada (NSERC) [SAPIN-2026-00047and SAPIN-2024-00026].

[1] STAR, L. Adamczyk *et al.*, Nature **548**, 62 (2017), 1701.06657.
[2] Z.-T. Liang and X.-N. Wang, Phys. Rev. Lett. **94**, 102301 (2005), nucl-th/0410079, [Erratum: Phys.Rev.Lett. 96, 039901 (2006)].
[3] Z.-T. Liang and X.-N. Wang, Phys. Lett. B **629**, 20 (2005), nucl-th/0411101.
[4] STAR, B. I. Abelev *et al.*, Phys. Rev. C **76**, 024915 (2007), 0705.1691, [Erratum: Phys.Rev.C 95, 039906 (2017)].
[5] STAR, M. S. Abdallah *et al.*, Phys. Rev. C **104**, L061901 (2021), 2108.00044.
[6] ALICE, S. Acharya *et al.*, Phys. Rev. C **101**, 044611 (2020), 1909.01281, [Erratum: Phys.Rev.C 105, 029902 (2022)].
[7] STAR, J. Adam *et al.*, Phys. Rev. C **98**, 014910 (2018), 1805.04400.
[8] STAR, M. I. Abdulhamid *et al.*, Phys. Rev. C **108**, 014910 (2023), 2305.08705.
[9] STAR, B. E. Aboona *et al.*, Phys. Lett. B **870**, 139891 (2025), 2505.05046.
[10] F. Becattini, V. Chandra, L. Del Zanna, and E. Grossi, Annals Phys. **338**, 32 (2013), 1303.3431.
[11] R.-h. Fang, L.-g. Pang, Q. Wang, and X.-n. Wang, Phys. Rev. C **94**, 024904 (2016), 1604.04036.
[12] F. Becattini and F. Piccinini, Annals Phys. **323**, 2452 (2008), 0710.5694.
[13] B. Betz, M. Gyulassy, and G. Torrieri, Phys. Rev. C **76**, 044901 (2007), 0708.0035.
[14] F. Becattini, L. Csernai, and D. Wang, Phys. Rev. C **88**, 034905 (2013), 1304.4427, [Erratum: Phys.Rev.C 93, 069901 (2016)].
[15] L. Csernai, V. Magas, and D. Wang, Phys. Rev. C **87**, 034906 (2013), 1302.5310.
[16] I. Karpenko and F. Becattini, Eur. Phys. J. C **77**, 213 (2017), 1610.04717.
[17] Y. Xie, D. Wang, and L. P. Csernai, Phys. Rev. C **95**, 031901 (2017), 1703.03770.
[18] H. Li, L.-G. Pang, Q. Wang, and X.-L. Xia, Phys. Rev. C **96**, 054908 (2017), 1704.01507.
[19] Y. Sun and C. M. Ko, Phys. Rev. **C96**, 024906 (2017), 1706.09467.
[20] S. Shi, K. Li, and J. Liao, Phys. Lett. B **788**, 409 (2019), 1712.00878.
[21] X.-L. Xia, H. Li, Z.-B. Tang, and Q. Wang, Phys. Rev. C **98**, 024905 (2018), 1803.00867.
[22] S. Shi, H. Zhang, D. Hou, and J. Liao, (2019), 1910.14010.
[23] B. Fu, K. Xu, X.-G. Huang, and H. Song, Phys. Rev. C **103**, 024903 (2021), 2011.03740.
[24] A. Lei, D. Wang, D.-M. zhou, B.-H. Sa, and L. P. Csernai, Phys. Rev. C **104**, 054903 (2021), 2110.13485.
[25] V. E. Ambrus and M. N. Chernodub, Eur. Phys. J. C **82**, 61 (2022), 2010.05831.
[26] O. Vitiuk, L. V. Bravina, and E. E. Zabrodin, Phys. Lett. B **803**, 135298 (2020), 1910.06292.
[27] J.-H. Gao, G.-L. Ma, S. Pu, and Q. Wang, Nucl. Sci. Tech. **31**, 90 (2020), 2005.10432.
[28] X.-Y. Wu, C. Yi, G.-Y. Qin, and S. Pu, Phys. Rev. C **105**, 064909 (2022), 2204.02218.
[29] F. Becattini *et al.*, (2024), 2402.04540.
[30] HADES, R. Abou Yassine *et al.*, Phys. Lett. B **835**, 137506 (2022), 2207.05160.
[31] X.-G. Deng, X.-G. Huang, Y.-G. Ma, and S. Zhang, Phys. Rev. C **101**, 064908 (2020), 2001.01371.
[32] Y. B. Ivanov, Phys. Rev. C **103**, L031903 (2021), 2012.07597.
[33] X.-G. Deng, X.-G. Huang, and Y.-G. Ma, Phys. Lett. B **835**, 137560 (2022), 2109.09956.
[34] C. Yi, S. Pu, L.-G. Pang, G.-Y. Qin, and X.-N. Wang, (2026), 2603.27521.
[35] K.-J. Sun *et al.*, Phys. Rev. Lett. **134**, 022301 (2025).
[36] D.-N. Liu *et al.*, (2025), 2508.12193.
[37] Y.-P. Zheng *et al.*, (2025), 2509.15286.
[38] J. Xu, (2026), 2602.23793.
[39] Y. Hidaka, S. Pu, and D.-L. Yang, Phys. Rev. **D97**, 016004 (2018), 1710.00278.
[40] S. Y. F. Liu and Y. Yin, Phys. Rev. D **104**, 054043 (2021), 2006.12421.
[41] F. Becattini, M. Buzzegoli, and A. Palermo, Phys. Lett. B **820**, 136519 (2021), 2103.10917.
[42] S. Y. F. Liu and Y. Yin, JHEP **07**, 188 (2021), 2103.09200.

[43] B. Fu, S. Y. F. Liu, L. Pang, H. Song, and Y. Yin, Phys. Rev. Lett. **127**, 142301 (2021), 2103.10403.

[44] F. Becattini, M. Buzzegoli, G. Inghirami, I. Karpenko, and A. Palermo, Phys. Rev. Lett. **127**, 272302 (2021), 2103.14621.

[45] C. Yi, S. Pu, and D.-L. Yang, Phys. Rev. C **104**, 064901 (2021), 2106.00238.

[46] S. Ryu, V. Jupic, and C. Shen, Phys. Rev. C **104**, 054908 (2021), 2106.08125.

[47] W. Florkowski, A. Kumar, A. Mazeliauskas, and R. Ryblewski, Phys. Rev. C **105**, 064901 (2022), 2112.02799.

[48] M. Buzzegoli, F. Becattini, G. Inghirami, I. Karpenko, and A. Palermo, Acta Phys. Polon. Supp. **16**, 39 (2023), 2208.04449.

[49] F. Becattini, Rept. Prog. Phys. **85**, 122301 (2022), 2204.01144.

[50] A. Palermo, E. Grossi, I. Karpenko, and F. Becattini, Eur. Phys. J. C **84**, 920 (2024), 2404.14295.

[51] STAR, J. Adam *et al.*, Phys. Rev. Lett. **123**, 132301 (2019), 1905.11917.

[52] STAR, M. Abdulhamid *et al.*, Phys. Rev. Lett. **131**, 202301 (2023), 2303.09074.

[53] ALICE, S. Acharya *et al.*, Phys. Rev. Lett. **128**, 172005 (2022), 2107.11183.

[54] S. A. Voloshin, EPJ Web Conf. **171**, 07002 (2018), 1710.08934.

[55] S. Y. F. Liu, Y. Sun, and C. M. Ko, Phys. Rev. Lett. **125**, 062301 (2020), 1910.06774.

[56] H.-Z. Wu, L.-G. Pang, X.-G. Huang, and Q. Wang, Nucl. Phys. A **1005**, 121831 (2021), 2002.03360.

[57] H.-Z. Wu, L.-G. Pang, X.-G. Huang, and Q. Wang, Phys. Rev. Research. **1**, 033058 (2019), 1906.09385.

[58] X.-L. Xia, H. Li, X.-G. Huang, and H. Z. Huang, Phys. Rev. C **100**, 014913 (2019), 1905.03120.

[59] F. Becattini, G. Cao, and E. Speranza, Eur. Phys. J. C **79**, 741 (2019), 1905.03123.

[60] H. Li, X.-L. Xia, X.-G. Huang, and H. Z. Huang, Global hyperon polarization and effects of decay feeddown, in *19th International Conference on Strangeness in Quark Matter*, 2021, 2108.04111.

[61] Y. B. Ivanov, V. D. Toneev, and A. A. Soldatov, Phys. Rev. C **100**, 014908 (2019), 1903.05455.

[62] Y. Guo, J. Liao, E. Wang, H. Xing, and H. Zhang, Phys. Rev. C **104**, L041902 (2021), 2105.13481.

[63] A. Ayala, I. Domínguez, I. Maldonado, and M. E. Tejeda-Yeomans, Phys. Rev. C **105**, 034907 (2022), 2106.14379.

[64] STAR, J. Adam *et al.*, Phys. Rev. Lett. **126**, 162301 (2021), 2012.13601, [Erratum: Phys.Rev.Lett. 131, 089901 (2023)].

[65] X.-L. Sheng, L. Oliva, Z.-T. Liang, Q. Wang, and X.-N. Wang, Phys. Rev. D **109**, 036004 (2024), 2206.05868.

[66] J.-p. Lv, Z.-h. Yu, X.-w. Li, and Z.-t. Liang, (2026), 2603.15135.

[67] Z. Zhang, J.-p. Lv, Z.-h. Yu, and Z.-t. Liang, Phys. Rev. D **110**, 074019 (2024), 2406.03840.

[68] Y.-G. Yang, R.-H. Fang, Q. Wang, and X.-N. Wang, Phys. Rev. **C97**, 034917 (2018), 1711.06008.

[69] X.-L. Sheng, L. Oliva, and Q. Wang, Phys. Rev. D **101**, 096005 (2020), 1910.13684, [Erratum: Phys.Rev.D 105, 099903 (2022)].

[70] X.-L. Xia, H. Li, X.-G. Huang, and H. Zhong Huang, Phys. Lett. B **817**, 136325 (2021), 2010.01474.

[71] D. Wagner, N. Weickgenannt, and E. Speranza, Phys. Rev. Res. **5**, 013187 (2023), 2207.01111.

[72] X.-L. Sheng, S.-Y. Yang, Y.-L. Zou, and D. Hou, Eur. Phys. J. C **84**, 299 (2024), 2209.01872.

[73] B. Müller and D.-L. Yang, Phys. Rev. D **105**, L011901 (2022), 2110.15630, [Erratum: Phys.Rev.D 106, 039904 (2022)].

[74] J.-p. Lv, Z.-h. Yu, Z.-t. Liang, Q. Wang, and X.-N. Wang, Phys. Rev. D **109**, 114003 (2024), 2402.13721.

[75] M. Wei and M. Huang, Chin. Phys. C **47**, 104105 (2023), 2303.01897.

[76] W.-B. Dong, Y.-L. Yin, X.-L. Sheng, S.-Z. Yang, and Q. Wang, Phys. Rev. D **109**, 056025 (2024), 2311.18400.

[77] A. Kumar, B. Müller, and D.-L. Yang, Phys. Rev. D **108**, 016020 (2023), 2304.04181.

[78] X.-L. Sheng, S. Pu, and Q. Wang, Phys. Rev. C **108**, 054902 (2023), 2308.14038.

[79] J. Chen, Z.-T. Liang, Y.-G. Ma, and Q. Wang, Sci. Bull. **68**, 874 (2023), 2305.09114.

[80] X.-L. Sheng, L. Oliva, Z.-T. Liang, Q. Wang, and X.-N. Wang, Phys. Rev. Lett. **131**, 042304 (2023), 2205.15689.

[81] J.-H. Chen, Z.-T. Liang, Y.-G. Ma, X.-L. Sheng, and Q. Wang, Sci. China Phys. Mech. Astron. **68**, 211001 (2025), 2407.06480.

[82] F. Li and S. Y. F. Liu, (2022), 2206.11890.

[83] X.-L. Sheng, Y.-Q. Zhao, S.-W. Li, F. Becattini, and D. Hou, Phys. Rev. D **110**, 056047 (2024), 2403.07522.

[84] X.-L. Sheng, X.-Y. Wu, D. H. Rischke, and X.-N. Wang, Phys. Rev. Lett. **136**, 082301 (2026), 2508.03496.

[85] B. Müller and A. Schäfer, Phys. Rev. D **98**, 071902 (2018), 1806.10907.

[86] Y. Guo, S. Shi, S. Feng, and J. Liao, Phys. Lett. **B798**, 134929 (2019), 1905.12613.

[87] M. Buzzegoli, Nucl. Phys. A **1036**, 122674 (2023), 2211.04549.

[88] K. Xu, F. Lin, A. Huang, and M. Huang, Phys. Rev. D **106**, L071502 (2022), 2205.02420.

[89] H.-H. Peng, S. Wu, R.-j. Wang, D. She, and S. Pu, (2022), 2211.11286.

[90] T. Lu, EPJ Web Conf. **364**, 03001 (2026).

[91] STAR, K. H. Ackermann *et al.*, Nucl. Instrum. Meth. A **499**, 624 (2003).

[92] L. Pang, Q. Wang, and X.-N. Wang, Phys. Rev. C **86**, 024911 (2012), 1205.5019.

[93] L.-G. Pang, H. Petersen, and X.-N. Wang, Phys. Rev. C **97**, 064918 (2018), 1802.04449.

[94] X.-Y. Wu, G.-Y. Qin, L.-G. Pang, and X.-N. Wang, Phys. Rev. C **105**, 034909 (2022), 2107.04949.

[95] J. Weil *et al.*, Phys. Rev. C **94**, 054905 (2016), 1606.06642.

[96] A. Schäfer *et al.*, Phys. Rev. D **99**, 114021 (2019), 1902.07564.

[97] J. Mohs, S. Ryu, and H. Elfner, J. Phys. G **47**, 065101 (2020), 1909.05586.

[98] J. Hammelmann, A. Soto-Ontoso, M. Alvioli, H. Elfner, and M. Strikman, Phys. Rev. C **101**, 061901 (2020), 1908.10231.

[99] J. Mohs, M. Ege, H. Elfner, and M. Mayer, Phys. Rev. C **105**, 034906 (2022), 2012.11454.

[100] SMASH, A. Schäfer, I. Karpenko, X.-Y. Wu, J. Hammelmann, and H. Elfner, Eur. Phys. J. A **58**, 230 (2022), 2112.08724.

[101] G. Inghirami and H. Elfner, Eur. Phys. J. C **82**, 796 (2022), 2201.05934.

[102] C. Yi *et al.*, Phys. Rev. C **109**, L011901 (2024), 2304.08777.
[103] I. A. Karpenko, P. Huovinen, H. Petersen, and M. Bleicher, Phys. Rev. C **91**, 064901 (2015), 1502.01978.
[104] A. Monnai, B. Schenke, and C. Shen, Phys. Rev. C **100**, 024907 (2019), 1902.05095.
[105] A. Monnai, B. Schenke, and C. Shen, Int. J. Mod. Phys. A **36**, 2130007 (2021), 2101.11591.
[106] F. Becattini, I. Karpenko, M. Lisa, I. Upsal, and S. Voloshin, Phys. Rev. C **95**, 054902 (2017), 1610.02506.
[107] H. Li, X.-L. Xia, X.-G. Huang, and H. Z. Huang, Phys. Lett. B **827**, 136971 (2022), 2106.09443.